COBEM 2023 27TH INTERNATIONAL CONGRESS OF MECHANICAL ENGENEERING

ABCM Brazilian Society of Mechanical Sciences and Engineering
27th ABCM International Congress of Mechanical Engineering
December 04-08, 2023, Florianópolis-SC, Brazil

COBEM 2023-1124
ETHANOL-WATER MIXTURES AS A PROMISING FUEL ALTERNATIVE FOR REDUCING HARMFUL EMISSIONS IN SPARK IGNITION ENGINE

Heron de Castro Ibraim[1]
Victor Pereira Toledo [1]
Elisângela Martins Leal[2]
Thales Leonardo Santos[2]

[1] Graduate Program of Mechanical Engineering, [2] Department of Mechanical Engineering, School of Mining, Federal University of Ouro Preto. Campus Morro do Cruzeiro, S/N, Bauxita, Ouro Preto, Minas Gerais, Brazil
e-mail:heron.ibraim@aluno.ufop.edu.br; victor.pt@aluno.ufop.edu.br; elisangelamleal@ufop.edu.br; thales.leonardo@aluno.ufop.edu.br

Abstract. *Ethanol emerges as a promising eco-friendly fuel choice for spark ignition engines, thanks to its diminished carbon footprint and potential to curb harmful emissions. This research employs Diesel RK software to conduct a technical examination of integrating ethanol into a gas-optimized spark ignition engine. The study delves into the impact of varying ethanol blends (E96, E90, E80, and E70) on OC13 engine performance and fuel efficiency. The results unveil that employing ethanol-water mixtures as fuel leads to decreased consumption. Furthermore, a marginal dip in engine power and torque accompanies the utilization of higher ethanol blends, while fuel consumption experiences a slight uptick. Altogether, the technical analysis demonstrates the promise of ethanol-water blends as a feasible fuel alternative. These findings serve as valuable insights for advancing alternative fuel technologies and their integration within the transportation sector.*

Keywords: *Ethanol fuel, Spark ignition engines, Diesel RK software, Ethanol-water mixtures, Exhaust emission.*

1. INTRODUCTION

The internal combustion engine stands as one of the primary energy conversion devices that have profoundly shaped modern transportation and industrial processes across the globe. Over more than four decades, Brazil has consistently employed ethanol fuel, solidifying its status as a pioneer in advocating and embracing ethanol as an alternative fuel source for transportation (Siciliano, 2022). Nevertheless, the combustion process associated with ethanol and conventional fuels generates polluting emissions that adversely impact air quality and contribute to global warming (Lius, 2023). Therefore, there is a pressing need to develop technologies that not only reduce polluting gas emissions but also enhance the overall efficiency of internal combustion engines. In this context, the use of biofuels, particularly ethanol, has emerged as a viable alternative, offering the potential to reduce the reliance on fossil fuels. Opting for hydrated alcohol over anhydrous alcohol further simplifies the production process, making it both easier and more cost-effective to obtain. This paper aims to analyze computationally the use of hydrated ethanol to optimize these systems of internal combustion engines.

The internal combustion engine comprises several integral components, including the piston, connecting rod, crankshaft, and valves, all of which must work in harmony for optimal performance. Computational analysis emerges as a powerful tool to simulate engine behavior and assess its performance under diverse operating conditions. This analytical approach enhances the understanding of the combustion process and facilitates the identification of potential improvements in engine design.

Ethanol, derived from renewable sources such as sugar cane, corn, and beet, has garnered global attention as a biofuel capable of curbing polluting gas emissions. However, the integration of ethanol as a fuel may require adjustments to the fuel injection system and engine design to ensure efficient combustion. Ethanol's high laminar flame velocity significantly contributes to improved thermal efficiency in engines (Savelenko, 2022). Its rapid burning rate permits a more efficient conversion of fuel energy into mechanical work, ultimately resulting in increased thermal efficiency (Ayad, 2021). This unique characteristic of ethanol combustion proves advantageous in extracting the maximum energy from the fuel, thereby enhancing overall engine performance.

As the demand for cleaner and less polluting fuels surges, ethanol emerges as a renewable biofuel with significant promise, particularly as an alternative to fossil fuels in internal combustion engines, spanning both light and heavy vehicles, including trucks (Mohammed, 2021). Nevertheless, the utilization of ethanol in truck engines presents formidable technical challenges owing to its physicochemical properties, such as low energy density and a propensity to absorb moisture from the air. Effectively addressing these challenges entails adapting the fuel injection system and other engine components to ensure proper performance and energy efficiency (Aleiferis, 2022).

2. MATERIALS AND METHODS

Within this system, the simplifying assumption that the working fluid behaves as an ideal gas and that the processes occur in a steady state, with negligible kinetic and potential energy, is assumed. The system boasts a compression ratio of 14.0:1, while the initial conditions stipulate an inlet pressure of 0.1 MPa and a temperature of 15ºC. To comprehensively analyze this system, the ideal gas law is employed, as elucidated by Eq. (1).

$$P\,V = m\,R\,T \tag{1}$$

In the context of this analysis, the variables are defined as follows: P represents the pressure of the working fluid, V stands for the volume of the working fluid, m denotes the mass of the working fluid, R signifies the specific constant unique to the working fluid, and T represents the temperature of the working fluid. Given that the processes under examination unfold in a state of equilibrium, it is assumed that the mass of the working fluid remains constant throughout the entire cycle. To determine the specific gas constant R, it is required the knowledge of the molar mass of the working fluid. Additionally, the compression ratio serves as a parameter for calculating the volume at the culmination of the compression process, denoted as V2, and it hinges on the initial volume, represented as V1. The compression ratio, CR, is mathematically defined as shown in Eq. (2).

$$CR = V_1/V_2 \tag{2}$$

In the realm of internal combustion engine analysis, the determination of heat release is executed by leveraging the chemical energy inherent in the fuel. This is achieved through the application of the single-zone combustion model, a methodology that aligns with the principles of the first law of thermodynamics, as succinctly represented by Equation (3).

$$\frac{dQ}{dt} - \frac{dW}{dt} + \sum \dot{m}_i h_i = \frac{dU}{dt} \tag{3}$$

Equation (3) delineates the process of computing heat release in open systems. In this equation, (dQ/dt) signifies the heat transferred per unit time across the system boundaries, (dW/dt) represents the work performed due to changes in the system boundaries, $(\dot{m}_i)$ denotes the mass flow entering and exiting the system boundaries, h_i stands for the enthalpy of the mass as it enters and exits the system boundaries, and (dU/dt) characterizes the rate of change of internal energy within the system (Heywood, 1988).

Within the realm of internal combustion engines, practical considerations necessitate the introduction of assumptions into the real cycle analysis, all while keeping the theoretical cycle as a reference point. These assumptions become imperative due to factors like non-uniform air-fuel mixture distribution, the presence of residual gases from prior cycles, heat dissipation from the combustion chamber, and disparate rates of heat dispersion.

In the single-zone model, the calculation of heat release relies on average values within the cylinder's volume. It is presumed that the cylinder filling operates under thermodynamic and chemical equilibrium conditions. Furthermore, this model assumes that both fuel vapor and combustion products within the cylinder adhere to ideal gas properties. Notably, any potential leaks from the piston, rings, or cylinder walls into the crankcase are disregarded for simplicity and model efficiency.

$$\frac{dQ_{net}}{dt} = \frac{dQ_{gr}}{dt} - \frac{dQ_{ht}}{dt} = p\frac{dV}{dt} + \frac{dU}{dt} \tag{4}$$

$$\frac{dQ_{net}}{dt} = \frac{Cp}{R}\left(p\frac{dV}{dt} + V\frac{dp}{dt}\right) - V\frac{dp}{dt} \tag{5}$$

$$\frac{dQ_{gr}}{dt} = \frac{Cp}{R}\left(p\frac{dV}{d\theta} + V\frac{dp}{d\theta}\right) - V\frac{dp}{d\theta} + \frac{dQ_{ht}}{d\theta} \tag{6}$$

Where: (dQ_{net}/dt) is the net rate of heat release, $\left(dQ_{gr}/dt\right)$ is the total heat release, (dQ_{ht}/dt) is the rate of heat transfer to the cylinder walls, and (dU/dt) is the change in internal energy of the charge is equal to the work done on the piston in the cylinder. After the necessary adjustments to the Eq. (4), it can be expressed in terms of the crankshaft angle (Eq. 6) instead of the time dependent variation.

Equation (6), $\left(dQ_{gr}/dt\right)$ signifies the overall rate of heat release, where Cp represents the specific heat capacities, R signifies the specific constant, p signifies the cylinder pressure, $(dV/d\theta)$ stands for the derivative of displacement

concerning crankshaft angle, and V represents the cylinder volume, $(dp/d\theta)$ signifies the derivative of cylinder pressure concerning crankshaft angle and $(dQ_{ht}/d\theta)$ denotes the rate of heat transfer to the cylinder walls.

Exergy represents the maximum potential work achievable within a system, and it can be categorized into two distinct forms as described in Eq. (7). One form is physical exergy, which encompasses mechanical and thermal work, while the other is chemical exergy, inherent to the chemical reactions occurring within the system (Bejan A. 2016).

$$Ex = Ex_{phy} + Ex_{che} \tag{7}$$

$$\frac{dEx}{d\theta} = \dot{E}x_{Che} - \dot{E}x_{W} \tag{8}$$

Once exergy values have been established, it becomes imperative to examine the exergy balance equation for each distinct exergy component. By merging the principles of the first and second laws of thermodynamics and accounting for the system's exergies, we can derive the exergy balance equation solved concernin the crankshaft angle, denoted as $(dEx/d\theta)$ in Equation (8). Here, $\dot{E}x_{Che}$ represents the rate of change of chemical energy, and $\dot{E}x_{W}$ signifies the rate of change of work exergy.

Equations (9) and Eq. (10) play a role in determining efficiency parameters. In this context, ε_1 represents the exergy efficiency in internal combustion engines, where (W_i/Ex_{fuel}) signifies the gross work output indicated by the fuel, relative to the chemical exergy input to the system. On the other hand, for a broader system perspective, ε_2 introduces a definition of exergy efficiency in internal combustion engines. It takes into account the exhaust exergy of the engine, which is particularly pertinent in contemporary engine systems where recuperating exhaust waste heat holds significance. Additionally, Eq. (10) stands as a valuable tool for quantifying the exergy efficiency of the system. This efficiency can be computed by discerning the disparities in exergy between both mechanical and thermal work and the exergy content of the fuel (Cesur, 2022).

$$\varepsilon_1 = \frac{W_i}{Ex_{fuel}} \tag{9}$$

$$\varepsilon_2 = \frac{Ex_w + Ex_{ex}}{Ex_{fuel}} \tag{10}$$

The study utilized a six-cylinder, turbocharged, four-stroke, water-cooled OC13 101 engine. Table 1 presents the engine's technical specifications, which were used for simulation purposes.

Table 1. Technical specifications of the engine.

Parameters	**Unit**	**Value**
Engine		OC13 101
Piston diameter	mm	130
Stroke	mm	160
Cylinder number		6
Stroke volume	dm^3	12.7
Effective power	kW	302
Compression ratio		12.6
Cooling type		Water
Fuel type		gas

Ethanol fuel, a biofuel primarily composed of ethanol alcohol derived from renewable sources, is denoted by designations such as E96, E90, E80, and E70, followed by percentages indicating ethanol content in the fuel. Notably, anhydrous ethanol contains minimal water content, while hydrous ethanol has a higher water content. The ethanol percentage, as exemplified by E96 (containing 96% ethanol and 4% water), serves as a reference point. In Table 2, comprehensive data for the mathematical model of natural gas, E96 (96% ethanol and 4% water), E90 (90% ethanol and 10% water), E80 (80% ethanol and 20% water), and E70 (70% ethanol and 30% water) are presented. These data encompass crucial fuel properties, including mass fractions, low heating values, density, thermal capacity at injector temperature, and molecular mass. These parameters are indispensable for conducting simulations, analyzing engine performance, and predicting emissions across diverse combustion systems employing varying fuel blends.

Table 2. The properties of Ethanol and Natural Gas.

Fuel properly	Natural Gas	E96	E90	E80	E70
Carbon (mass fractions)	0.753	0.753	0.4997	0.475	0.4466
Hydrogen (mass fractions)	0.246	0.246	0.1305	0.1295	0.1285
Oxygen (mass fractions)	0	0.3559	0.3698	0.3954	0.4249
Sulfur content	0	0	0	0	0
Low Heating Value of fuel (MJ/kg)	49.74	26.27	25.59	24.32	22.87
Density (kg/m^3) (1)	0.748	1.868	1.798	1.682	1.565
Fuel Thermal Capacity at a temperature of the injector (J/(kg*K)	2114	1680	1687	1699	1712
Molecular Mass of fuel	16.74	44.95	43.26	40.46	37.65
Fuel temperature (K)	380	380	380	380	380

(1) measured at 323 K

3. RESULT AND DISCUSSION

3.1 Engine torque, effective power, in-cylinder pressure, and temperature

Figures 1 and 2 are instrumental in validating the model by juxtaposing the model's predicted engine torque and power outputs with the actual performance data from the OC13 101 engine, as furnished in SCANIA's manufacturer documentation. This rigorous comparison between the model's predictions and the manufacturer's empirical data served as a critical benchmark to gauge the model's precision and dependability. The validation process, highlighting the remarkable congruence between predicted and actual torque and power values, unequivocally affirmed the model's suitability for subsequent analysis and experimentation, thereby enhancing the overall credibility of the research findings and conclusions.

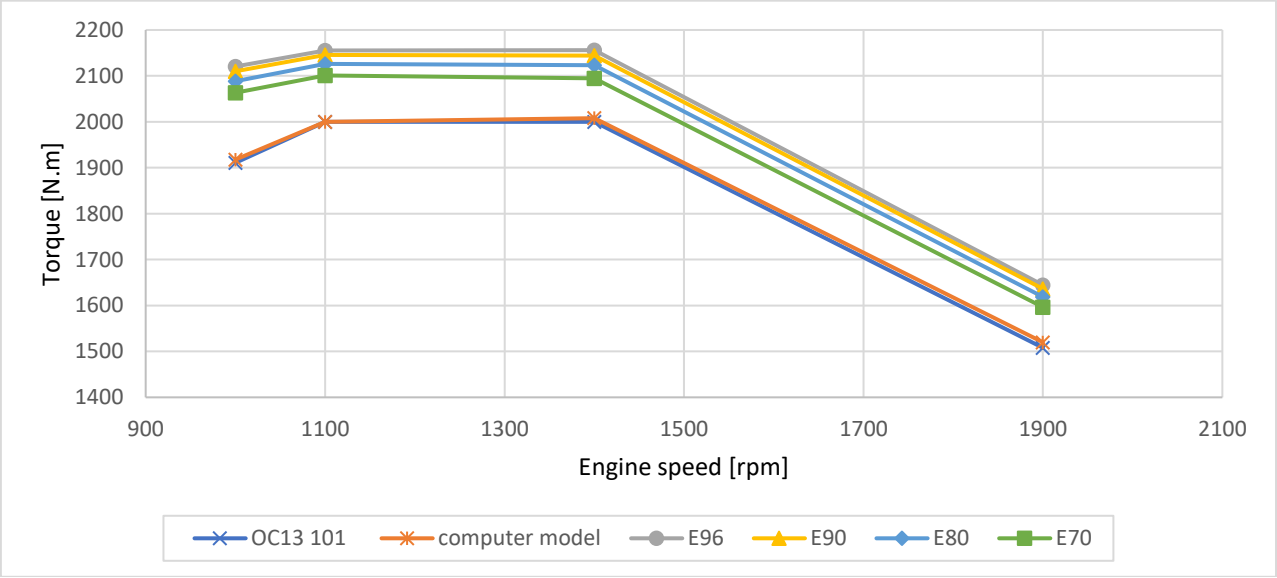

Figure 1. Engine brake torque values and percentage change in the different blend of fuel rates in the engine.

Figure 1 delineates engine torque values and their percentage variations across diverse fuel types in a gas engine setup. The outcomes reveal a consistent trend of reduced engine torque in comparison to the standard engine at all engine speeds when using the fuel-water mixture. The most significant torque reduction, standing at 2.9%, is observed at 1900 rpm when employing E70. This decline stems from the lower calorific value inherent in the water mixture, resulting in diminished energy output during combustion. Conversely, Figure 1 spotlights the notable performance enhancement achieved through E96 injection. This particular fuel blend engenders an upswing in engine torque across all speed ranges, with peak torque realized at 1400 rpm. The introduction of new enthalpy via the injected water into the combustion chamber contributes to this torque improvement. The heightened surface tension of water facilitates superior fuel atomization, fostering a more homogenous mixture with air and an accelerated combustion process. These dynamics culminate in heightened combustion efficiency and, consequently, improved engine performance without any detriment.

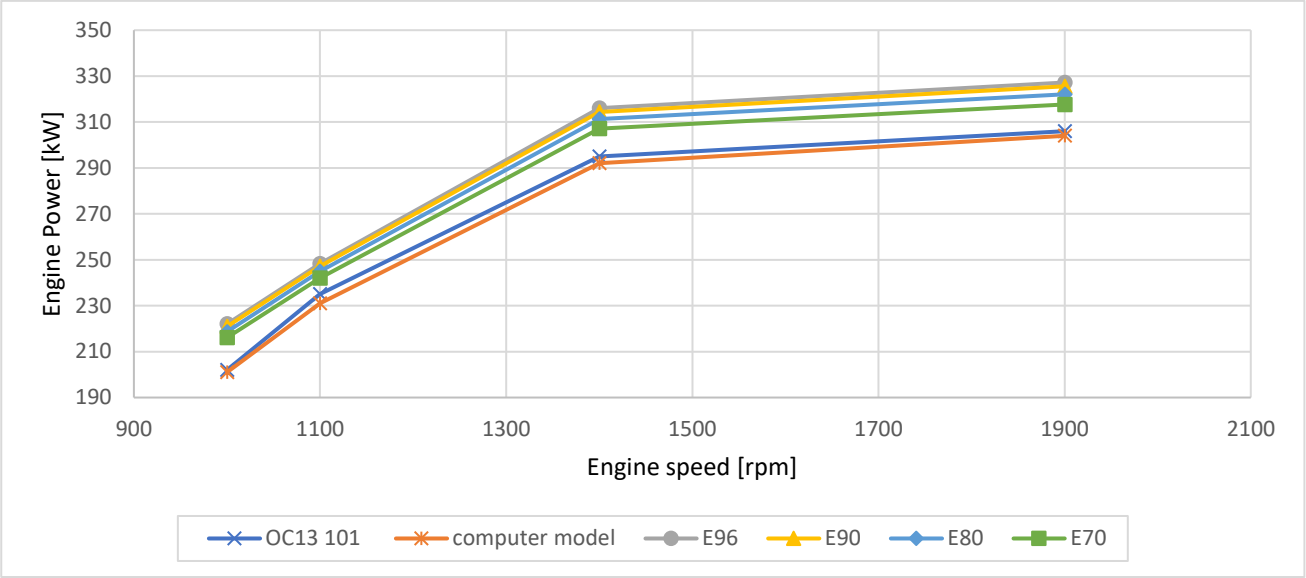

Figure 2. Engine brake power values and percentage change in the different blends of fuel rates in the engine.

Figure 2 illustrates the change in engine power when employing E96 fuel, with the maximum effective power increase recorded at 1900 rpm. Figures 1 to 4 serve as sources of insights into the influence of fuel-water mixtures on engine performance metrics and combustion characteristics.

In Figure 3, in-cylinder pressure values obtained under full-load conditions are presented. This figure delineates the impact of using E80 fuel across different engine speeds. Particularly, E80 leads to a decrease in in-cylinder pressure compared to the standard configuration, primarily due to ethanol's lower calorific value. Conversely, employing E96 at various engine speeds results in increased in-cylinder pressure compared to the standard scenario. This rise can be attributed to enhanced combustion efficiency, improved air-fuel mixture homogeneity, and an accelerated combustion rate.

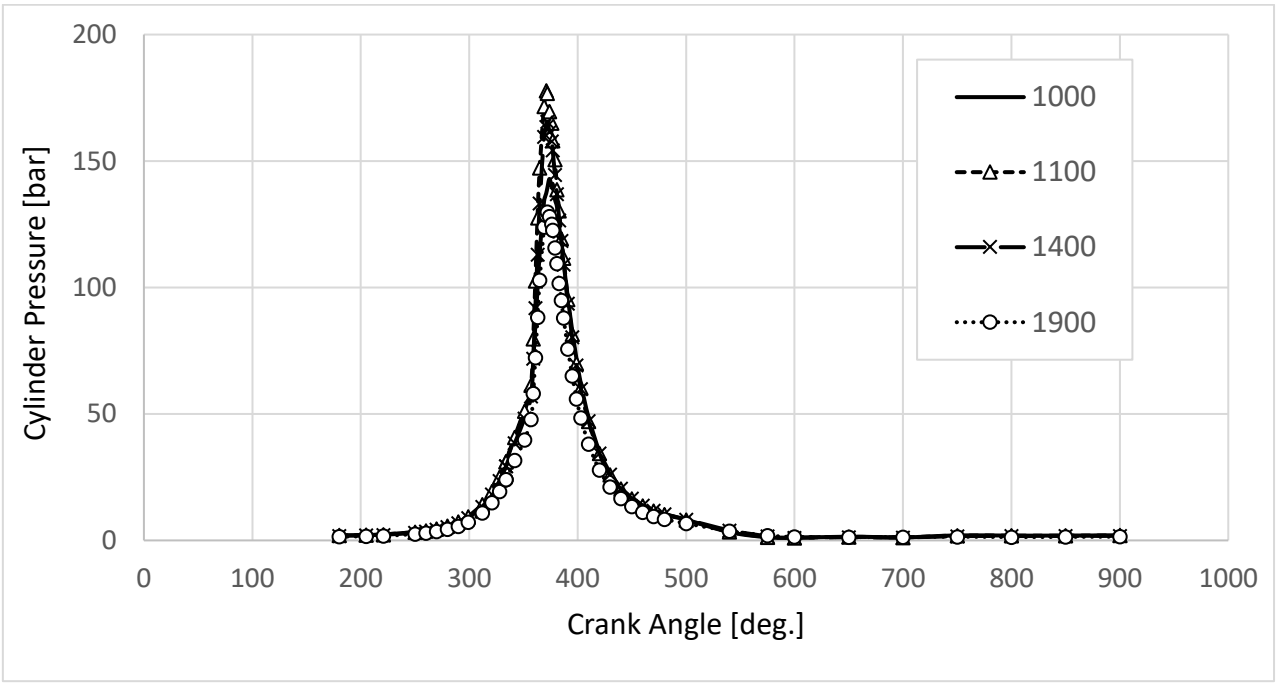

Figure 3. In-cylinder pressure changes of different engine speeds to the E80 fueled engine.

Figure 4 provides insights into the heat release characteristics under full-load conditions, offering a comparative view between the optimal engine speed rates and standard conditions. When employing E80 fuel, a discernible reduction in heat release is observed owing to its lower calorific value, resulting in diminished heat dissipation. Nevertheless, this

inherent limitation is effectively counterbalanced by the favorable influence of water injection, which bolsters the combustion rate and expedites combustion reactions. As engine speed escalates, the accelerated combustion reactions facilitated by water injection effectively compensate for the decreased heat release associated with E80 fuel. This synergistic interplay engenders tangible improvements in engine performance and efficiency, rendering the utilization of E80 fuel in conjunction with water injection a compelling strategy for optimizing combustion processes within internal combustion engines. In summary, these findings underscore the potential of alternative fuels as proactive measures for curbing pollutant emissions while concurrently preserving or even enhancing key engine performance parameters.

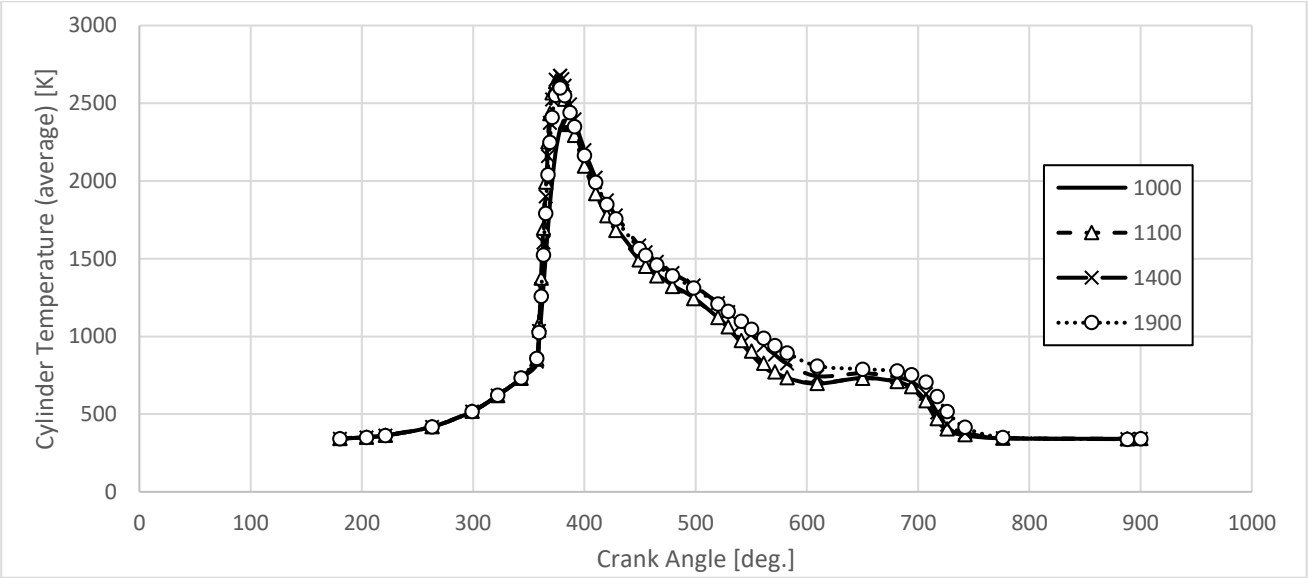

Figure 4. Temperature changes of different engine speeds to the E80 fueled engine.

3.2 Engine fuel mass flowrate and Specific Fuel Consumption

Figure 5 offers a visualization of the relationship between the combustion quantity within the engine and the water content within ethanol fuel. The graph unequivocally illustrates that the inclusion of water in ethanol yields noteworthy cost savings by reducing the demand for pure ethanol in the fuel blend. This cost-effective advantage renders water-infused ethanol an enticing choice for optimizing engine performance while simultaneously bolstering economic efficiency. Notably, the figure underscores E80, representing a fuel blend comprising 80% ethanol and 20% water, as the most favorable option. E80 stands out as it necessitates a reduced volume of pure ethanol compared to alternative fuel mixtures, such as E96 (96% ethanol and 4% water), E90 (90% ethanol and 10% water), and E70 (70% ethanol and 30% water).

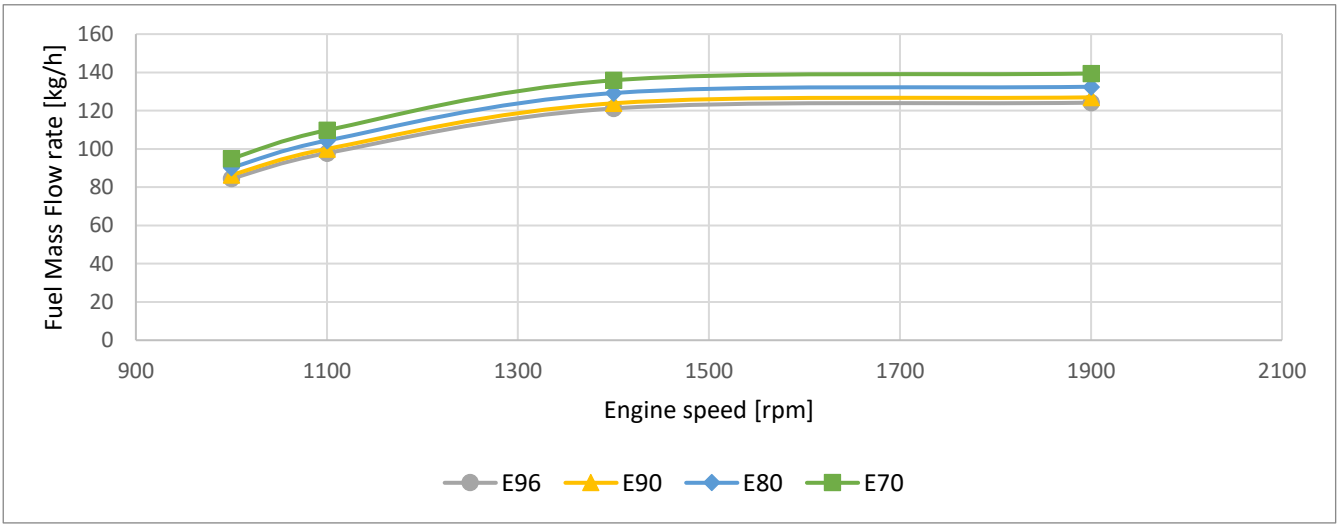

Figure 5. Relationship between Fuel mass flow rate and engine speed for the analyzed fuels.

By adopting E80 as the primary fuel, the overall cost of the ethanol fuel blend is diminished, all the while upholding the desired performance and emission characteristics. This underscores the viability of incorporating water into ethanol as a cost-effective strategy, without compromising the suitability of the fuel for engine operation. Thus, based on the insights unveiled in Figure 5, E80 emerges as the most cost-efficient choice, minimizing the requirement for pure ethanol while delivering the sought-after benefits of ethanol as a fuel.

Meanwhile, Figure 6 portrays a distinct enhancement in engine-specific fuel consumption across all engine speeds when water becomes a constituent of the fuel mixture. This performance boost is attributed to the high oxygen content within water, facilitating the formation of hydroxyl radicals during combustion. These hydroxyl radicals, in turn, catalyze heightened combustion efficiency and reaction rates, fostering a more effective energy release. Furthermore, the presence of water fosters rapid and efficient flame propagation within the cylinder, facilitating swifter and more effective combustion. This phenomenon translates into improved air-fuel mixture homogenization and enhanced combustion efficiency, ultimately elevating engine performance. The confluence of these factors underscores water injection into the engine as a valuable approach to augment combustion and attain elevated levels of efficiency within internal combustion engines.

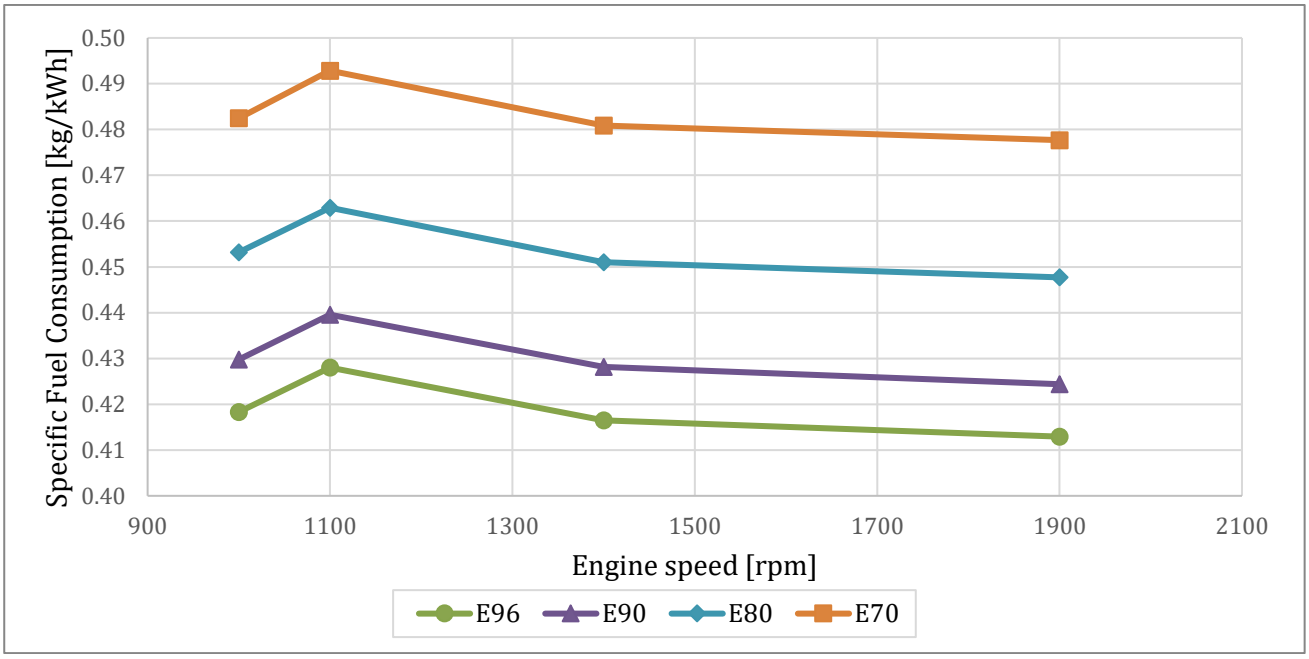

Figure 6. Specific fuel consumption values and percentages at different rates in the engine.

4. CONCLUSION

In this study, the primary focus is centered on enhancing engine performance and concurrently curbing pollution emissions in a spark ignition engine through the application of alternative fuels with varying water content. Different fuel blends comprising ethanol and water, encompassing E96 (4% water), E80 (20% water), E90 (10% water), and E70 (30% water) are studied. Particularly, the findings elucidated that E70 fuel, while resulting in a marginal dip in engine torque and effective power, demonstrated promising attributes. In the case of the thermal capacity of the fuels, the analysis reveals a significant 11.65% reduction in energy conversion for E70 compared to the performance achieved by E96. Remarkably, the disparity narrows substantially when E80 is compared, showcasing a much more modest 6.94% difference. However, the results of the E80 fuel blend exhibited a noteworthy 1.5% increase in engine torque at 1400 rpm. This achievement can be attributed to the synergistic effect of water and ethanol injection, capitalizing on the initial pressure surge during fuel ignition to elevate peak mean effective pressure within the cylinder.

Furthermore, the exploration into hydrated ethanol, while not groundbreaking in the Brazilian automotive landscape, underscores its potential significance. The quest for an optimal ethanol hydration ratio holds the promise of optimizing the renewable energy potential within the matrix. Concurrently, it has the potential to render ethanol more cost-effective, particularly by alleviating the expenses associated with the dehydration process during production. Looking ahead, future endeavors may unveil additional environmental benefits, potentially including a reduction in pollutant emissions like nitrous oxides. This effect can be attributed to the thermal Zeldovich phenomenon, where water's involvement contributes to a moderated chamber temperature, a factor that warrants exploration and holds the promise of a greener automotive future.

5. ACKNOWLEDGEMENTS

The authors acknowledge PROPEM (Graduate Program of Mechanical Engineering) of the Federal University of Ouro Preto (UFOP). Also, this work was carried out with the support of the Coordination for the Improvement of Higher Education Personnel - Brazil (CAPES).

6. REFERENCES

Lei, J., Li, J., Liu, Y., 2022, Ethanol drop impingement on ultracold surfaces under low-temperature cold-start conditions of engines, Fuel, Vol. 311, pp.122573.

Siciliano, B., Silva, C. M., Melo, T. C. C., Vicentini, P. C., Arbilla, G., 2022, An analysis of speciated hydrocarbons in hydrous ethanol (H100) and ethanol-gasoline blend (E22) for vehicle exhaust emissions, Atmospheric Environment, Vol. 285, pp.119248.

Roy, S., Mishra, R., Askari, O., Jarrahbashi, D., 2023, Reduced ethanol skeleton mechanism for multi-dimensional engine simulation, Journal of the Energy Institute, Vol. 106, pp.101147.

Aleiferis, P.G., Shukla, J., Brewer, M., Cracknell, R.F., 2022, Effect of water content in ethanol on spray formation at subcooled and flash-boiling conditions, International Journal of Heat and Mass Transfer, Vol. 182, pp.121884.

Bejan A., 2016, Advanced engineering thermodynamics. 4th ed. John Wiley & Sons, Inc.

Ayad, S. M. M. E., Vago, C. L., Belchior, C. R. P., Sodré, J. R., 2021, Cylinder pressure-based calibration model for engines using ethanol, hydrogen, and natural gas as alternative fuels, Energy Reports, Vol. 7, pp. 7940-7954.

Loyte, A., Suryawanshi, J., Bhiogade, G., Devarajan, Y., Subbiah, G., 2022, Recent developments in utilizing hydrous ethanol for diverse engine technologies, Chemical Engineering and Processing - Process Intensification, Vol. 177, pp. 108985.

Mendiburu, A. Z., Lauermann, C. H., Hayashi, T. C., Mariños, D. J., Costa, R. B. R., Coronado, C. J. R., Roberts, J. J., Carvalho Jr., J. A., 2022, Ethanol as a renewable biofuel: Combustion characteristics and application in engines, Energy, Vol. 257, pp. 124688.

Savelenko, V. D., Ershov, M. A., Kapustin, V. M., Chernysheva, E. A., Abdellatief, T. M. M., Makhova, U. A., Makhmudova, A. E., Abdelkareem, M. A., Olabi A.G., 2022, Pathways resilient future for developing a sustainable E85 fuel and prospects towards its applications, Science of The Total Environment, Vol. 844, pp.157069.

Lius, B. H., Senthil, A., Mahendar, K., Mihaescu, M., Cronhjort, A., 2023, Energy and exergy characteristics of an ethanol-fueled heavy-duty SI engine at high-load operation using lean-burn combustion, Applied Thermal Engineering, Vol. 224, pp. 120063.

Cesur, I., 2022, Effects of water injection strategies on performance and exhaust emissions in an ethanol fueled gasoline engine, Thermal Science and Engineering Progress, Vol. 34, pp.101397.

Mohammed, M. K., Balla, H. H., Al-Dulaimi, Z. M. H., Kareem, Z. S., Al-Zuhariry M. S., 2021, Effect of ethanol-gasoline blends on SI engine performance and emissions, Case Studies in Thermal Engineering. Vol. 25, pp. 100891.

Onder voorbehoud van wijzigingenational, *NMS 1711-410Gas Onder voorbehoud van wijzigingenational*, bodybuilder.scania.com/content/dam/bodybuilder/tbb-files/belgium/fisches-techniques/motorenspecificaties---spécification-du-moteur/13/416+MS+Gas+1711.pdf. Accessed 02 May 2023.